THE WELDABILITY AND MECHANICAL BEHAVIOR OF MEDIUM CARBON STEEL IN CW Nd:YAG LASER WELDING

by Han-Sur Bang[1], Young-Pyo Kim[2]*, Seiji Katayama[3], Woong-Seong Chang[4] and Chang-Woo Lee[5]

[1]Division of Aerospace and Naval Architectural Engineering, Chosun University
375 Seosuk-dong, Dong-gu, Gwangju, 501-759, Korea, hsbang@mail.chosun.ac.kr
[2]Graduate Student of Chosun University, ypkim@stmail.chosun.ac.kr
[3] Joining and Welding Research Institute, Osaka University
11-1 Mihogaoka, Ibaraki, Osaka 567-0047, Japan, katayama@jwri.osaka-u.ac.jp
[4] Welding Research Center, Research Institute of Industrial Science & Technology
32 Hyoja-dong, Nam-gu, Pohang, Kyungbuk, 790-330, Korea, wschang@rist.re.kr
[5] Ulsan College
29 Mugeo-dong, Nam-gu, Ulsan, 680-749, Korea, cwlee@mail.ulsan-c.ac.kr

ABSTRACT

This paper describes the weldability and mechanical behavior of JIS S45C medium carbon steel (corresponding to KS SM45C and SAE 1045) for machine structures in CW Nd:YAG laser welding. In general, medium carbon steels have a limited application to the industrial fields in spite of good mechanical characteristics. This is due to welding difficulty because of the high carbon contents and impurities in this material. Therefore, in this study the laser weldability of medium carbon steel with adjusted contents of S and P has been investigated in order to extend the application to medium carbon steels. Several experiments and numerical simulations have been conducted to determine the characteristics of mechanical behavior in CW Nd:YAG laser welds. The results of the simulations concur with the experiment results. From the result of this study, the application possibility of CW Nd:YAG laser welding to medium carbon steel has been confirmed. Also, the appropriateness of mechanical behavior simulation has been verified to analyze and predict the welding phenomena.

KEYWORDS

Medium carbon steel, laser weldability, Nd:YAG laser, thermal elasto-plastic analysis, finite element method

1. Introduction

In general, medium carbon steels are utilized for axle, crankshaft, bolts, gear and parts of machines that require durability and an anti-abrasion property.

As carbon contents increase, the possibility of cracking (cold and hot) and porosity increase. Therefore, pre-heating (100～200℃) and post weld heat treatment (above 600～650℃) are necessary to prevent cold and hot cracking. To apply arc welding to medium carbon steels, it is necessary to use low-hydrogen welding rods and pre & post-heating treatments. Normally, recommended carbon content in conventional welding is below 0.2%[1].

On the other hand, lowering contents of impurity elements (S and P) which cause cracking can also be a useful method to control the occurrence of cracking, in view of metallurgy.

While investigating an example of laser application to medium carbon steel a laser has been utilized for surface hardening in the machinery parts. Laser welding to medium carbon steel has shown that welding is possible but may be subjected to cracking. This is due to the brittleness and low ductility of laser welds. However, relevant research on this topic is insufficient.

Therefore, the goal of the study is to extend the use of medium carbon steels in the industrial fields by application of laser welding. Chemical composition controlled material has been used to minimize solidification cracking. After an investigation on laser weldability with Nd:YAG laser system, numerical simulation on thermal elasto-plasticity has been conducted by using finite element method. Results from the experiment and simulation have been compared and examined.

2. Laser weldability

2.1 Experiment method

The welding specimen is S45C medium carbon steel (contents of P, S are adjusted to avoid hot cracks). The dimension of the specimen is pictured in Fig.1. A schematic diagram of the experiment set-up is pictured in Fig.2.

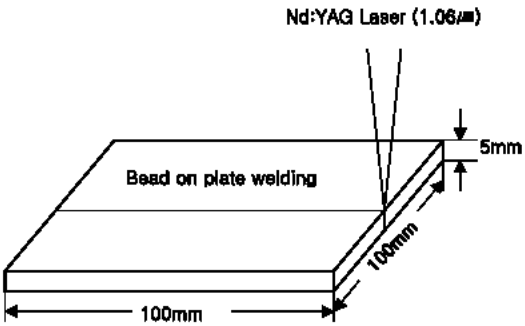

Fig.1 Dimension of specimen

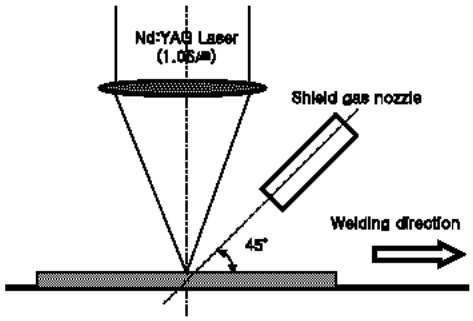

Fig.2 Schematic diagram of the experiment set-up

The chemical composition and the mechanical properties are shown in Table.1 and Table.2.

Table.1 Chemical composition. (wt%).

C	Si	Mn	P	S	Cu	Ni	Cr
0.45	0.22	0.78	0.009	0.004	0.02	0.02	0.08

Table.2 Mechanical properties

Y.S (Mpa)	T.S (Mpa)	Elong. (%)	R.A (%)	Hard. (HRB)
Min.490	Min.686	Min. 17	Min. 45	89

To conduct the experiment, high power CW Nd:YAG laser system (max. output power 3.5kW) is utilized. After cleaning with acetone and drying the specimen, bead-on-plate welding is applied to the 100(L)×100(B)×5(T) sized specimen without surface polishing. Ar gas (30ℓ /min) is used as a shield gas. Welding parameters such as travel speed and the depth of focus vary in order to determine fusion properties of CW Nd:YAG laser welding. After observing the porosities in the welded specimen with an X-Ray transmission imaging system (Fig.3), the shape of the weld bead and any welding defects, such as crack, spatter, undercut, etc., are observed with an optical microscope and an image analyzer to the specimen sectioned.

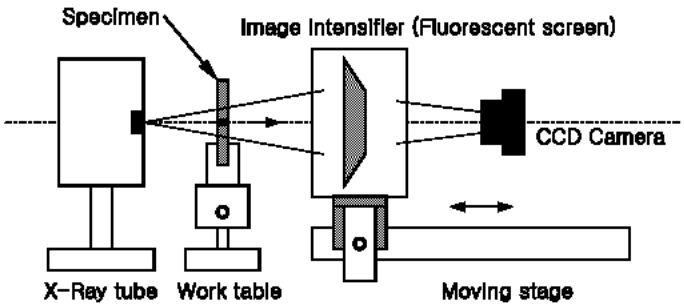

Fig.3 Schematic arrangement of X-Ray transmission imaging system for observation of porosity

2.2 Experiment result

The test results of CW Nd:YAG laser welding is shown in Table.3. When CW Nd:YAG laser welding is applied, the output power(3.3kW) and the focal depth(f_d) are fixed and the travel speed vary under the range of 12.5 ㎜/s ~100 ㎜/s. Penetration depth vs travel speed, and width vs travel speed diagrams are illustrated in Fig.4. Considering the results, the relation between travel speed and width and penetration depth is inversely

proportional and due to the heat input. This means the penetration depth and the width decreases if travel speed increases.

Table.3 Result at the different travel speed

Power (kW)	Travel speed (㎜/s)	f_d (㎜)	Penetration depth (㎜)	Width (㎜)
3.3	25	-5	3.1	2.95
		-2.5	3.7	2.85
		0	3.3	2.8
		+2.5	2.13	2.75

Table.4 Result at the different focal depth

Power (kW)	Travel speed (㎜/s)	f_d (㎜)	Penetration depth (㎜)	Width (㎜)
3.3	25	-5	3.1	2.95
		-2.5	3.7	2.85
		0	3.3	2.8
		+2.5	2.13	2.75

Table.4 shows the results when the output power (3.3kW) and travel speed (25 ㎜/s) are fixed and a varying focal depth is within the range of -5 ㎜ ~ +2.5 ㎜ in CW Nd:YAG laser welding. Fig.5 illustrates the relation between penetration depth vs focal depth and width vs focal depth. The penetration depth shows a maximum value in the range of focal depth, -2.5 ㎜ ~ 0 ㎜. The width has a tendency to become wide at the defocussed focal position. This is due to a reduction of energy density in the laser beam.

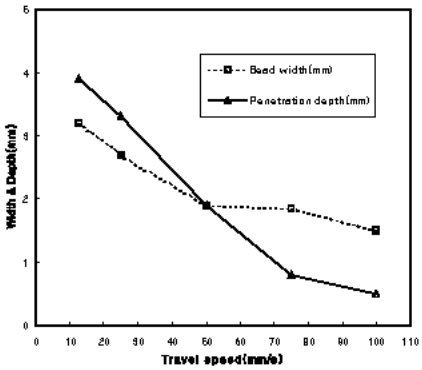

Fig.4 Effect of travel speed on penetration depth and width

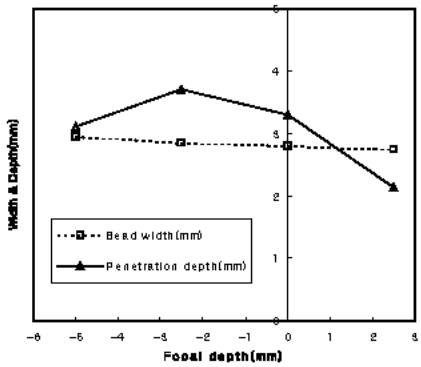

Fig.5 Effect of focal depth on penetration depth and width

From the observation of bead surface, cross section and x-ray image, welding defects (spatter, undercut and crack) do not appear to the whole test condition except porosity. Fig.6 illustrates the amount of porosity per unit length (1 ㎝) caused by a varying travel speed and focal depth. As travel speed increases, the occurrence of porosities decreases which is caused by a reduction of heat input. Porosities are observed primarily below the center of the welding cross section. The largest amount of porosity appears at a focal depth of 0 ㎜. As the focal depth is distant from 0 ㎜, the occurrence of porosity decreases as a result of the reduction of heat input. Porosities are observed primarily below the center of the welding cross section.

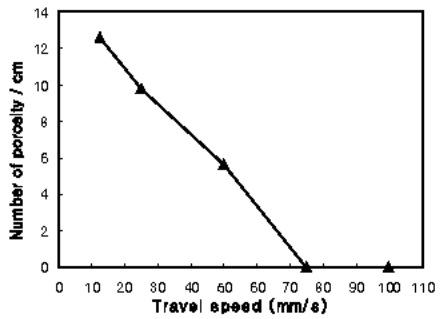

(a) Variation of travel speed

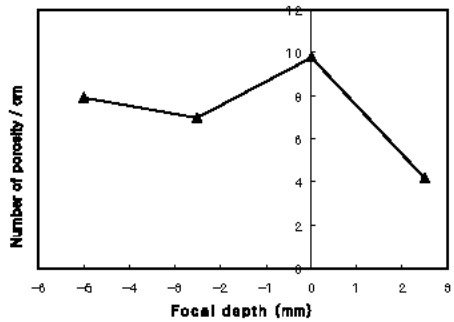

(b) Variation of focal depth

Fig.6 Effect of travel speed and focal depth on the number of porosity

Established research results in the mild steel are shown in Fig.7. Absorptivities of carbon steel at different wavelength 1.06 ㎛ and 10.6 ㎛ are 0.09 and 0.03 respectively[2]. By comparing the results, the following is estimated:

- Nd:YAG laser is more profitable to the steel welding than CO_2 laser.
- As carbon contents increases, the penetration depth of laser welding decreases.

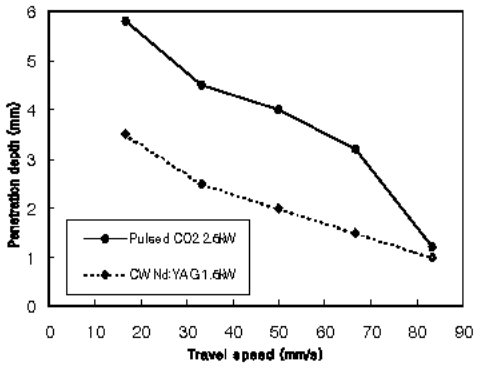

Fig.7 Effect of travel speed on penetration depth at mild steel

3. Mechanical behavior in CW Nd:YAG laser welding

3.1 Modeling and temperature distribution

Authors have conducted finite element analysis on working condition of P=3.3kW and V=12.5 ㎜/s to analyze two-dimensional unstationary heat conduction problem. Welding heat source is assumed as an instantaneous heat source. Two dimensional four-node isoparametric elements are used to find the value at the node and element as well as any integral point. This adopts the natural coordinate, which uses the same interpolative function to the displacement and the element coordinate.

Fig.8 and Fig.9 show the physical coefficients of the material and mechanical properties, which are depending on temperature.

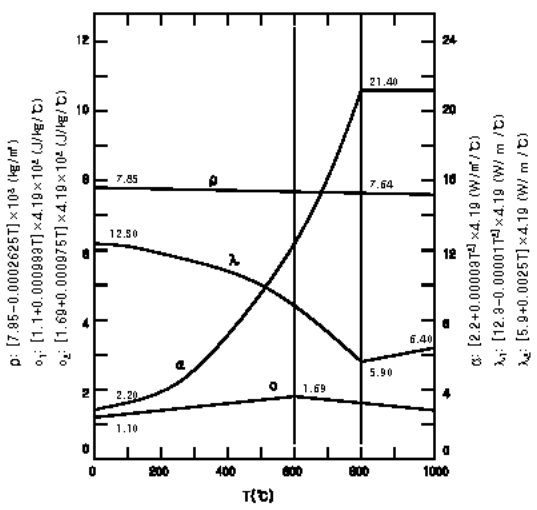

Fig.8 Temperature dependency of physical properties used heat conduction analysis

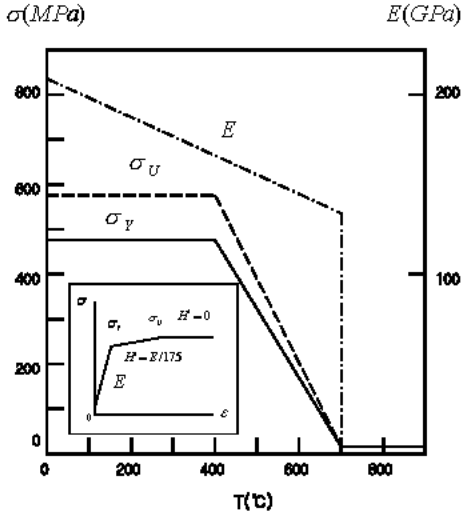

Fig.9 Temperature dependency of mechanical properties used thermal stress analysis

The material is assumed as an isotropic material. The work-piece is initially at 20℃. Convective flow in the weld pool, vaporization in the keyhole and radiation heat transfer is not considered. In order to analyze the thermal elasto-plasticity, a self-developed finite element code is used. This code has been verified to provide the accurate result of simulation in the case of conventional arc welding [4]

The attenuation of beam power according to the Beer-Lambert's law is described by

$$P = P' \exp(-\alpha L) \qquad (1)$$

For a laser welding, the heat input [5], Q, is determined from the following equation:

$$Q = \eta_L \frac{P}{V} \qquad (2)$$

The schematic mesh division and the principle dimensions of the model for analysis are shown in Fig.10. The number of nodes and elements are 4,029 and 3,900 respectively. The minimum size of an element is 0.1 ㎜× 0.1 ㎜.

Fig.10 Schematic mesh division (two-dimensional half model).

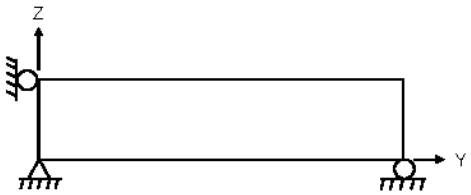

Fig.11 Boundary condition for stress analysis

The results of the simulation to the cooling time and rate in weld metal are 0.95 sec and 3.15×10^2℃/sec respectively for $\Delta T_{800/500}$. In the case of $\Delta T_{1,200/500}$, cooling time and rate are 1.25 sec and 5.58×10^2℃/sec.

The simulation results of temperature distribution in weld metal and HAZ are shown in Fig.12. Temperature distribution along the width direction is shown in Fig.13. The temperature is observed at z=0.1 ㎜ from the surface since extreme temperature change occurs at that position. The material is assumed to recover its mechanical stiffness below 700℃.

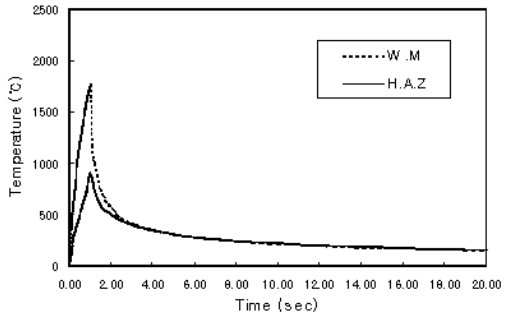

Fig.12 Comparison of the temperature distribution between weld metal and HAZ

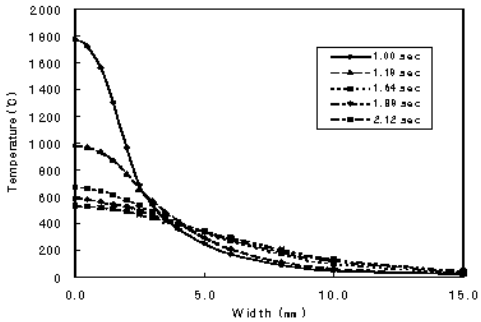

Fig.13 Temperature distribution along the width direction

Fig.14 shows the heat distribution after 1sec by using isothermal layer. The comparisons between experiment and simulation to the HAZ line are illustrated in Fig.15.

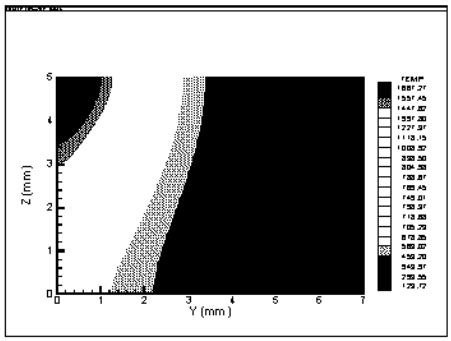

Fig.14 Heat distribution after 1sec

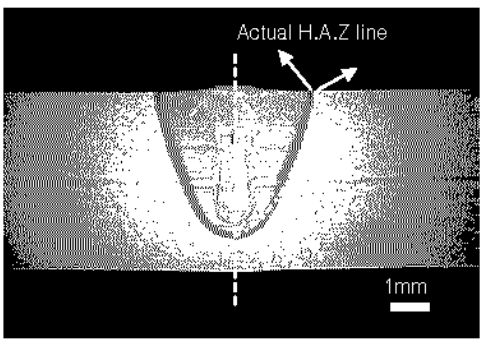

Fig.15 Comparison between experiment and simulation on the HAZ line

As shown in the figure, above simulation results are well in accord with the experiment results.

3.2 Characteristics of distribution of residual stresses and plastic strains

Using temperature distributions calculated in the previous chapter, two-dimensional thermal elasto-plastic analysis has been performed. Boundary condition of analyzed model is shown in Fig.11. Based on the result, the characteristics of distributions of welding residual stresses and plastic strains are to be clarified in this chapter.

Shown in Fig.16 is the distributions of residual stresses and plastic strains along the y-axis at the position z= 0.1 ㎜. The components of residual stresses, σ_x and σ_y, which are produced in the weld metal and HAZ are tensile. Another component of residua stresses σ_z is too small. The residual plastic strain component ε_x^p along the y-axis is small compressive in the weld metal and HAZ. The component ε_y^p along the y-axis is compressive in the weld metal and HAZ, but tensile in the base plate. The plastic strain component ε_z^p is largely tensile in the weld metal and HAZ.

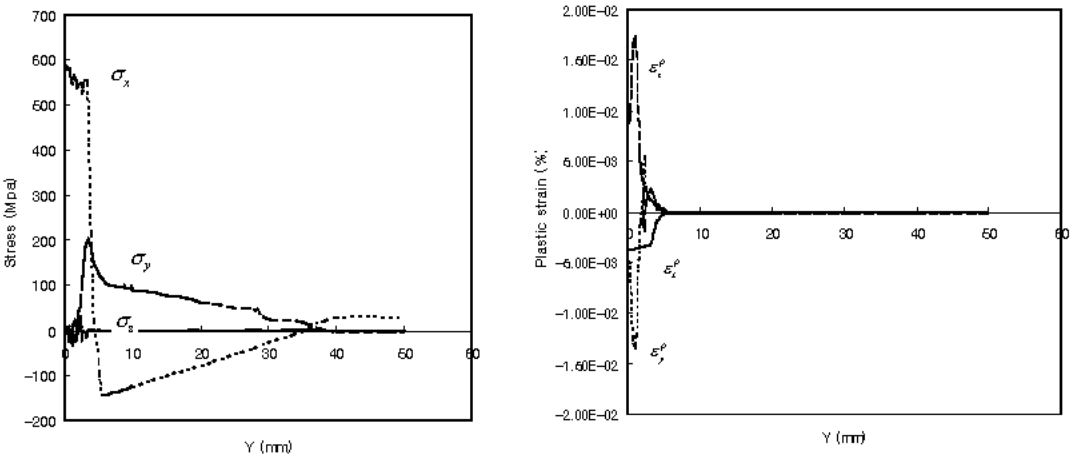

Fig.16 Distributions two-dimensional residual stresses and plastic strains in y-direction

4. Conclusions

From the results of experiment and numerical simulation, authors could confirm the possibility of Nd:YAG laser welding to the medium carbon steel and predict the mechanical behavior in welds through the thermal elasto-plastic analysis. Residual stresses and plastic strains in welds are small as respect the general characteristics of laser welding.

Acknowledgements

This work was supported by the Brain Korea 21 project in 2001.

References

[1] ASM, Metals Handbook: 8th Edition, Vol.6, p.187-199.

[2] W. W. Duley, Laser Welding: John Willy & Sons, Inc.1999, p.25-66, p.114-136.

[3] S. Katayama and A. Matsunawa: Proc. CISFFEL, IS, CEA & TWI, Toulon, France, Vol.1 (1998), p.215-222.

[4] H. S. Bang, J. M. Kim, C. S. Ro, S. J. Kim and W. S. Chang: Science and Technology of Welding and Joining (2001), Vol.6, No.4, p.213-219.

[5] K. W. Carlson: *ICALEO*'85, p.49-57

[6] U. Ueda, Y. C. Kim, T. Yamakita and H. S. Bang: Trans. of JWS, 6-1 (1988), p.47-52 (in Japanese)